J. Fluid Mech. (1971), *vol.* 48, *part* 2, *pp.* 229–239
Printed in Great Britain

The drag on oscillating flat plates in liquids at low Reynolds numbers

By CORNELIUS C. SHIH
The Research Institute, University of Alabama, Huntsville, Alabama
AND HARRY J. BUCHANAN
Aero-Astrodynamics Laboratory, Marshall Space Flight Center, NASA, Huntsville, Alabama

(Received 15 December 1969 and in revised form 13 January 1971)

An experimental investigation was conducted to describe the fluid flow about oscillating flat plates and to determine the magnitude and nature of forces acting on the plates at low Reynolds numbers. In the experiment, the Reynolds number was varied from 1·01 to 1057·0; three period parameters, 1·57, 2·07 and 4·71, were applied; two fluids, water and SAE 30 motor oil, and three flat plates of various sizes with or without end plates were used. The analysis of data resulted in graphical presentation of the relationships among the drag coefficient, the Reynolds number and period parameter. The drag coefficient becomes less dependent on the Reynolds number for values greater than 250. The relationship between the drag coefficient and period parameter is pronounced throughout the entire range of the Reynolds number tested.

Introduction

In the space flight of a liquid-fuelled rocket, the propellant usually oscillates or sloshes due to the motion of the vehicle. Damping of the sloshing propellant is considered an important part of the control system design. Usually, the damping is accomplished by the use of a series of baffles mounted inside the propellant tank.

A method of computing the damping or energy dissipation of a flat ring totally submerged in a viscous fluid which was contained in a cylindrical tank, was developed by Miles in 1958. The resulting equation has been used for calculating the damping under high g conditions in which the baffle drag coefficient was obtained from a series of experiments at moderately high Reynolds numbers. Under reduced gravity conditions, the theory by Satterlee & Reynolds (1964) shows that the sloshing frequency becomes small, resulting in a flow of low Reynolds number down to about unity. This finding has been substantiated by the flight of NASA's Uprated Saturn I (Buchanan & Bugg 1967) in which sloshing frequencies of less than 0·0033 cycles per second were observed for acceleration levels of the order of 0·02 cm/sec^2.

The application of Miles's method for calculating damping under low g conditions has been considered inappropriate because of the lack of knowledge

regarding the baffle drag coefficient at low Reynolds numbers. To the authors' knowledge, all other related studies made by Keulegan & Carpenter (1958), McNown & Keulegan (1959), Brater, McNown & Stair (1958), Morrison *et al.* (1950), Schwind, Scotti & Skogh (1964), and Cole & Gambucci (1961) are also concerned with relatively high Reynolds numbers about 6000 and above.

Therefore, a study was initiated to pursue the following objectives: experimentally determine the drag forces on two-dimensional oscillating flat plates at low Reynolds numbers; reduce the data in terms of relationships among the drag coefficient, Reynolds number and period parameter; observe and describe the flow phenomena about the oscillating flat plates; provide drag coefficient data in a proper form for establishing an equation for baffle damping at low Reynolds numbers.

In the experiment, instead of an oscillating flow with a fixed flat plate simulating the case of the sloshing propellant, a flat plate was oscillated because of the better control and more accurate measurement of the oscillation in the low Reynolds number range. Although the difference between forces produced by moving a submerged object through a fluid and those produced in submerging the object in a uniform stream of comparable characteristics has been shown by Lamb (1932, pp. 12–20) and others, this difference for the case of a flat plate can be proved to be negligibly small if the plate is relatively thin as shown by Buchanan (1968) and Batchelor (1967, pp. 404–9). Hence, this experimental approach is justifiably adapted for this study.

Experimental equipment and procedure

Using the apparatus illustrated in figure 1, experiments were performed on the drag coefficient of a flat plate oscillated in a direction normal to the plate in an incompressible viscous fluid at low Reynolds numbers. For all of the tests the liquid was contained in a rectangular glass-walled tank with inside dimensions 25·40 cm × 27·94 cm × 49·53 cm.

A variable speed electric motor was used to drive a scotch yoke mechanism which converted the rotary motion into a sinusoidal translation. By varying the motor speed, it was possible to vary the frequency of the translation from approximately 1 rad/sec up to 10 rad/sec. The scotch yoke was provided with an adjustable stroke, by means of which the amplitude of the motion could also be varied from 0 to 1·0 cm. With these variables it was possible to vary the maximum velocity during a cycle between 0 and 8·89 cm/sec. The plate was mounted on a sting extending downward from a moving carriage which was driven by the scotch yoke. The carriage itself consisted of a pair of rails which slid inside a corresponding set of bearings attached to the frame. This was to ensure that the motion of the plate was entirely translational. Two different fluids, water and SAE 30 motor oil, were used in the experiments to provide a wide range of Reynolds numbers.

All plates tested were constructed of 0·32 cm thick aluminium and had the following dimensions: (1) 20·32 cm × 2·54 cm, (2) 20·32 cm × 1·27 cm and (3) 20·32 cm × 1·27 cm, but with 4·13 cm diameter end plates for eliminating

three-dimensional effects. The plates were located approximately 12·60 cm from the tank bottom and 25·40 cm from either end. Preliminary tests in which these distances were varied showed no detectable wall or free surface interference until the plate was within one or two plate widths of the boundary. In the span-wise direction, a gap of approximately 2·54 cm was left on either side between the plate and the tank wall. Initially it was planned to have only a minimum of clearance between the plate and the tank walls, but interference effects made it necessary to shorten the plates and add end plates to eliminate three-dimensional effects.

For measuring the forces under 10 g, a sting supporting the plate was attached to an arm cantilevered from the moving carriage. Strain gauges were then attached to this arm providing a simple but sensitive means of measuring the force on the plate. Actually, two strain gauge arms were used in the tests: the smaller had a thickness of 0·09 cm and was used to measure forces ranging up

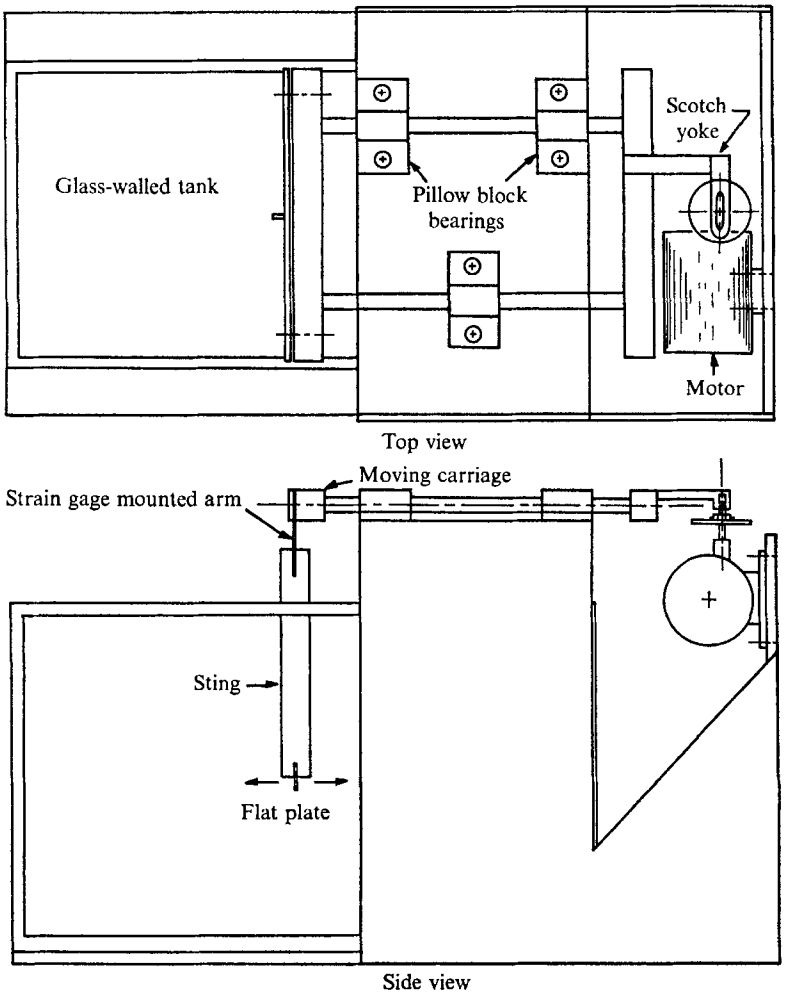

FIGURE 1. Experimental apparatus.

to 5 g force; the other had a thickness of 0·16 cm and was used in most of the cases. Both arms were made of carbon steel and were interchangeable. A pair of strain gauges (nominal gauge factor 2·0) were wired on each arm, one on either side, to form a half bridge and connected to a Budd strain indicator box for doubling the sensitivity as well as providing temperature compensation. The signal from the strain gauge system was then passed through a variable electronic filter in order to eliminate high frequency interference caused by the vibration of the cantilevered sting and plate. The first mode natural frequency of the sting determined by plucking the sting in air, was approximately 3·5 Hz and was almost identical with the frequency of the interference pattern. Because the frequency of the signal of interest was always less than 1 c/s, it was simple to isolate and remove the unwanted interference. The filtered signal was displayed on an oscilloscope.

In addition to the force measurements, motor rev/min was also recorded with an induction activated sensor which was so arranged to generate a blip signal each time the mechanism completed a half cycle. This signal was recorded also on the oscilloscope. Permanent records of these traces were made on photographs with a Polaroid camera.

This apparatus was calibrated from 0 to 10 gf by static loading using standard laboratory weights. The calibration signal was passed through the filter in the same fashion as for the actual tests and displayed on the oscilloscope for direct reading.

Presentation of experimental data

Because of the complexity of the flow phenomena, it was determined that the dimensional analysis might be the best available approach to the problem of the drag force exerted on an oscillating flat plate in a viscous fluid. By using the principles of dimensional analysis, a set of dimensionless parameters may be formed in an implicit function from pertinent quantities involved in this flow problem as follows:

$$\int \left(\frac{2F_d}{U_m^2 L W \rho}, \frac{U_m \tau}{W}, \frac{U_m \rho W}{\mu}, \frac{L}{W} \right) = 0, \tag{1}$$

where F_d denotes the drag force exerted on the oscillating flat plate, U_m the maximum velocity of the plate during a cycle, L the plate length, W the plate width, τ the period of oscillation, ρ the fluid density, μ the fluid viscosity. The first parameter in the function $\int$ of (1) is called the drag coefficient, C_d; the second parameter is a period parameter; the third parameter is the Reynolds number; and the last term is a geometric parameter.

A general form of the equation for the total force exerted on a submerged object in an unsteady flow, which consists of inertia force F_i and drag force F_d, is given by Morrison *et al.* (1950) as follows:

$$F = F_i + F_d = \rho C_m V_0 \, dU/dt + \tfrac{1}{2} C_d L W \rho U |U|, \tag{2}$$

where C_m and C_d are the coefficients of inertia and drag respectively, V_0 the object

volume, LW the effective area of the object, U the flow velocity. Analytical evaluation of the coefficients C_m and C_d can only be accomplished by solving the complete Navier–Stokes equations. While some analytical work has been done for non-oscillating laminar flow about a perpendicular plate, the problem becomes extremely difficult and has not been solved when oscillations are considered.

For an oscillating flow, it may be assumed that

$$U = -U_m \cos\theta, \tag{3}$$

where θ is the time-dependent angular displacement. In the case of an oscillating plate θ can be measured so that it is equal to zero for the central position of the plate. Combining (2) and (3) shows that the inertial force F_i and drag force F_d are out of phase for an angle of $\frac{1}{2}\pi$, signifying that, as F_i becomes zero, F then is entirely formed by F_d. In order to obtain the coefficients C_d and C_m for the oscillating flow empirically, Keulegan & Carpenter (1958) derived expressions of the coefficients through the Fourier analysis as given below:

$$C_d = -\frac{3}{4}\int_0^{2\pi} \frac{F\cos\theta}{\rho U_m^2 LW}\, d\theta, \tag{4}$$

$$C_m = \frac{2U_m T}{\pi^3 W}\int_0^{2\pi} \frac{F\sin\theta}{\rho U_m^2 LW}\, d\theta. \tag{5}$$

All quantities in the right-hand side of (4) and (5) are known or to be measured.

By evaluating the integrals in (4) and (5), values of C_d and C_m can be determined empirically. As pointed out by Keulegan & Carpenter, these coefficients are arbitrarily defined parameters and may be considered equivalent to the approximate averages of instantaneous values of the drag and inertial coefficients.

Since the drag force is predominant over the inertia force under the particular flow conditions of interest, and the inertia and drag forces are 90 degrees out of phase, the maximum total force occurs when the drag force is very near its maximum value and when the inertial force is nearly zero. This phenomenon is illustrated for test run 12 in figure 2. Therefore, C_d has been considered to be of main interest in this study.

In the evaluation of C_d, the use of (4) was found to be laborious. A simplified method of evaluating C_d has been developed by assuming that the maximum force is equal to the maximum drag force. Thus, an approximate value of C_d can be obtained by the following equation:

$$C_d = 2F/\rho U_m^2 LW, \tag{6}$$

where all quantities on the right-hand side of (6) are known or to be measured through experiments.

For a wide range of Reynolds numbers tested, drag coefficients which were obtained by using the two methods, compared favourably as shown in table 1.

Therefore, the simplified method was applied to reduce the bulk of data for C_d. It should be noted however that only a few values of the inertia coefficient, C_m, were found by this method because of the difficulty in determining experimentally the value of F_i.

In addition to C_d and C_m, the Reynolds number, $U_m \rho W/\mu$, and the period parameter $U_m \tau/W$ were calculated from the data reduction. In this study, $U_m = \eta\omega$ and $\tau = 2\pi/\omega$, where η is the amplitude of oscillation and ω the driving frequency.

Table 2 presents the calculated data for all 65 test runs. For runs 1 to 36 water was used as the test medium. A motor oil (SAE 30) was used for all other runs. End plates were added for all tests after run 29 for preventing end effects.

In order to visualize the flow field generated by the oscillating plate, a dye was injected near the plate. For the visualization, water was used and the end plates were removed from the model to provide a better view of the dye streaks.

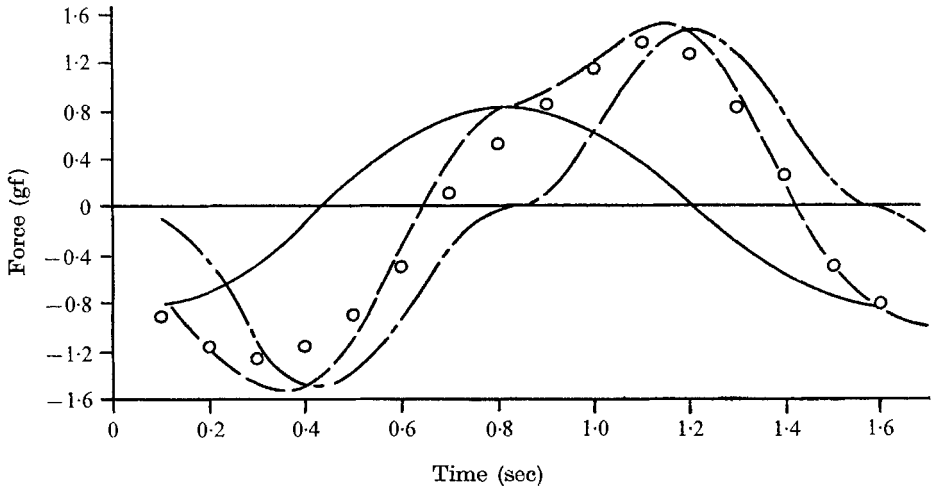

FIGURE 2. Comparison of calculated and experimental data for run 12. ○, experimental force; ——, calculated inertial force; — — —, calculated drag force; – – –, calculated total force.

Run no.	C_d by (4)	C_d by simplified method	Reynolds number
12	6·84	6·85	531
42	16·97	16·60	4·3

TABLE 1

Based on the analysis of photographed dye streaks, a series of sketches depicting the vortex flow field around the oscillating plate is presented in figure 3. The sequence of sketches in figure 3 illustrates the flow field as follows: (i) as the plate starts to move vortices are formed at the edge of the plate; (ii) at the end of the stroke the vortices are at their maximum size and are still attached; (iii) as the plate begins to move in the other direction, the old vortices are pushed aside and new vortices begin to form on the downstream side of the plate; (iv) the resulting vortex combination is U-shaped; (v) as the plate continues to move to the central position, the U-shaped vortices tend to break up into smaller vortices.

Run no.	ω (rad/sec)	Max. force (gf)	C_D	$\frac{U_m\tau}{W}$	$\frac{U_m W\rho}{\mu}$	Run no.	ω (rad/sec)	Max. force (gf)	C_D	$\frac{U_m\tau}{W}$	$\frac{U_m W\rho}{\mu}$
1	3·04	1·48	15·16	1·57	513	34	3·63	1·70	12·17	1·57	663
2	2·07	1·48	14·99	↓	354	35	2·55	1·01	14·65	↓	463
3	4·00	2·46	14·50	↓	685	36	1·47	0·36	15·67	↓	267
4	4·03	3·58	9·26	2·07	1057	37	5·28	4·26	14·71	4·71	5·57
5	2·92	1·90	9·34	↓	775	38	4·20	3·20	17·46	↓	4·43
6	1·73	0·75	10·50	↓	464	39	3·01	1·70	18·06	↓	3·18
7	4·05	1·30	6·64	↓	531	40	2·01	0·92	22·07	↓	2·13
8	3·17	0·72	6·05	4·71	414	41	1·01	0·33	31·67	↓	1·01
9	2·47	0·50	6·87	↓	323	42	4·08	2·87	16·60	↓	4·31
10	2·15	0·42	7·60	↓	281	43	2·32	1·25	22·36	↓	2·45
11	1·61	0·21	6·96	↓	210	44	5·15	3·54	11·21	↓	8·82
12	4·05	1·34	6·85	↓	531	45	7·13	6·48	10·69	↓	12·22
13	1·82	0·23	5·84	↓	229	46	9·37	9·66	10·59	↓	16·06
14	1·48	0·20	7·85	↓	186	47	6·19	5·14	11·18	↓	10·61
15	4·57	1·43	5·74	↓	575	48	7·85	6·35	8·65	↓	13·46
16	1·10	0·09	7·28	↓	139	49	4·47	1·54	16·63	2·07	17·24
17	2·28	0·40	6·42	↓	299	50	7·70	4·60	3·73	↓	17·24
18	1·97	0·30	6·58	↓	258	51	11·87	9·76	3·33	↓	42·92
19	2·16	0·38	6·92	↓	282	52	1·91	1·99	26·25	↓	3·65
20	1·98	0·34	7·29	↓	249	53	2·93	3·74	20·99	↓	5·60
21	1·98	0·31	6·64	↓	252	54	5·00	8·75	16·84	↓	9·56
22	3·08	0·64	5·67	↓	392	55	2·09	1·44	35·69	1·57	3·10
23	2·13	1·02	9·52	2·07	530	56	3·09	2·53	28·69	↓	4·58
24	2·35	1·20	9·17	↓	585	57	4·23	4·26	25·78	↓	6·27
25	1·53	0·55	9·87	↓	381	58	5·15	5·79	23·64	↓	7·63
26	2·16	1·02	9·21	↓	539	59	4·69	5·00	24·64	↓	6·95
27	1·75	0·64	8·80	↓	438	60	3·12	2·17	24·20	↓	9·06
28	1·31	0·46	11·21	↓	329	61	4·21	3·69	22·58	↓	11·93
29	5·11	2·00	6·42	4·71	643	62	5·13	5·12	21·07	↓	14·54
30	3·87	1·21	7·91	↓	483	63	6·28	7·40	20·32	↓	17·80
31	2·79	0·64	6·95	↓	348	64	7·21	10·06	20·96	↓	20·14
32	2·01	0·33	6·79	↓	251	65	5·15	5·17	21·13	↓	14·11
33	5·02	2·71	10·14	1·57	911						

TABLE 2. Calculated data

A nearly identical fluid behaviour was observed by Schwind *et al.* (1964) using a fixed plate in a sinusoidally varying stream.

The data in table 2 are presented in figures 4, 5 and 6 to graphically illustrate the findings of this study. Six values of C_m were plotted against the Reynolds number for a given period parameter of 4·71 and presented in figure 7.

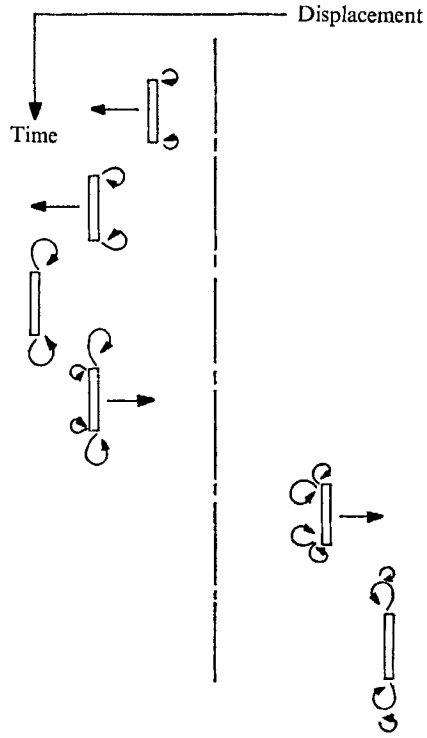

FIGURE 3. Sequence of sketches of flow field.

Discussion of experimental results and conclusions

Figure 4 compares the drag coefficient data as a function of the Reynolds number for cases with and without the end plates. Since no significant differences were observed for the two cases, it was deduced that three-dimensional effects were not appreciable in this problem. In any event the end plates were employed wherever possible and did appear to reduce the scattering of experimental data. Also indicated in this figure is the slight dependence of drag coefficient on Reynolds number over the range from 250 to 1000. The same observation was made by Keulegan & Carpenter (1958), although their findings only extended down to a Reynolds number of 4200. It appears then that for values of Reynolds number above 250, the drag coefficient is influenced primarily by the period parameter.

Figure 5 compares the new drag coefficient data with that of Keulegan & Carpenter's study as a function of period parameter. The Reynolds number is not constant in this figure but varies from point to point. All of these data were

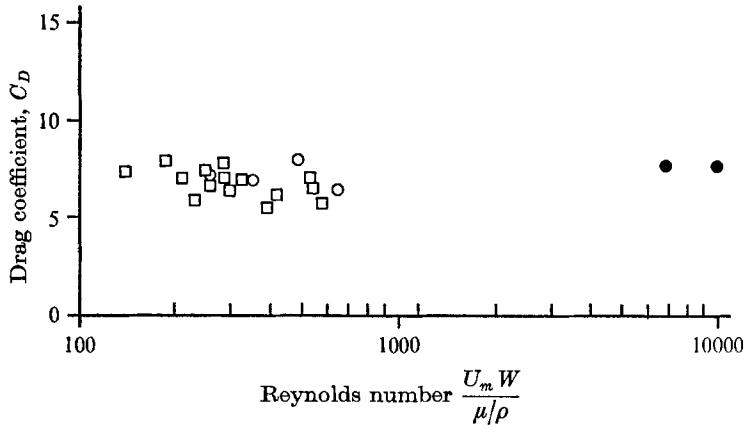

FIGURE 4. End effects on drag coefficient. ○, two-dimensional data (end plates); □, data without end plates; ●, two-dimensional data (Keulegan & Carpenter 1958). $U_m\tau/W = 4{\cdot}71$.

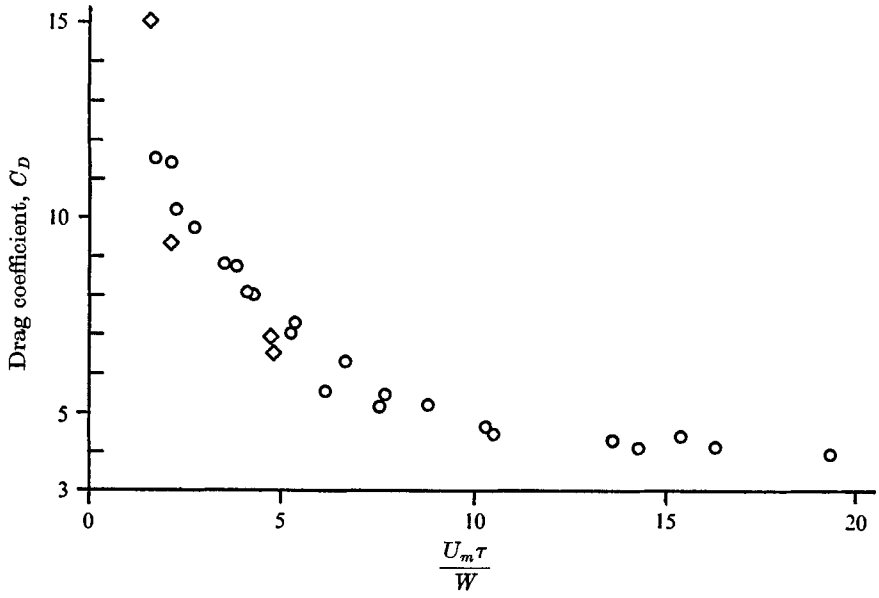

FIGURE 5. Existing data. ○, from Keulegan & Carpenter (1958); ◇, new.

selected from the high Reynolds number region previously described so that the data shown here should be only a function of period parameter. As indicated, data from these tests were in reasonable agreement with that obtained by Keulegan & Carpenter and exhibited the same variation with period parameter, $U_m\tau/W$.

Figure 6 presents all of the data from these tests. Drag coefficient C_d is shown to be a function of the Reynolds number and the period parameter $U_m\tau/W$. The curves drawn through the data in this figure were fitted by eye and show C_d to be relatively independent of the Reynolds number for values of the Reynolds

number greater than 250. Below this value the drag coefficient increases rapidly, suggesting a transition in the flow at this point. Unfortunately this could not be confirmed visually because the oil used for the low Reynolds number cases was

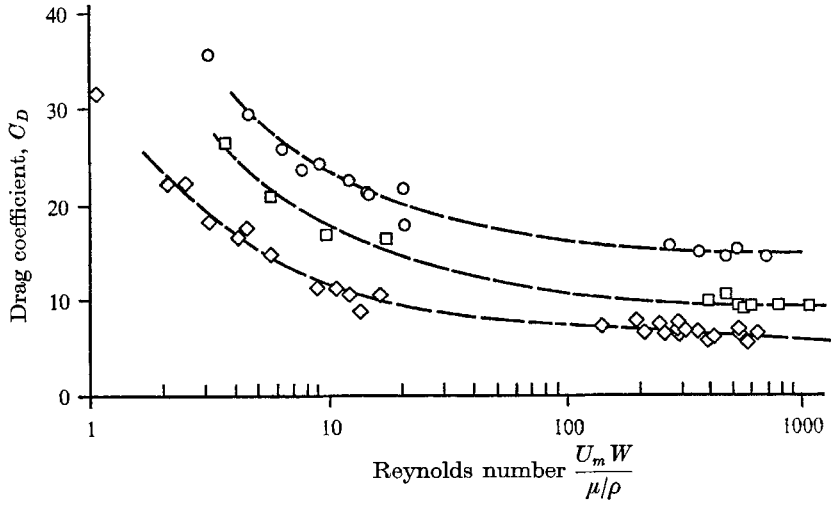

FIGURE 6. Drag coefficient as a function of Reynolds number. Values of $U_m T/W$: ○, 1·58; □, 2·07; ◇, 4·71.

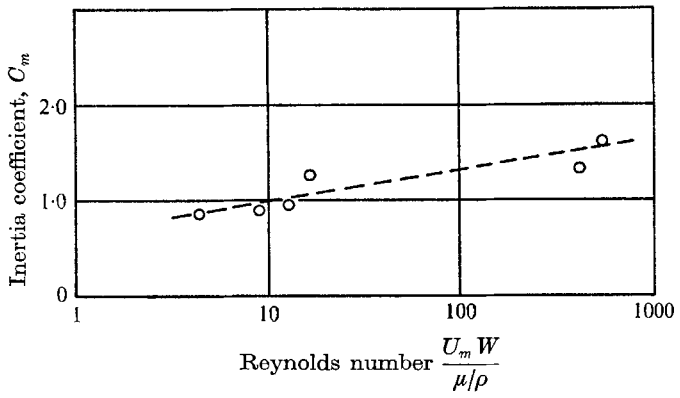

FIGURE 7. Inertia coefficient as a function of Reynolds number at period parameter of 4·71.

very dark and did not permit photography. However, it was distinctively noted that the relationship between the drag coefficient and period parameter is pronounced throughout the entire range of the Reynolds number tested.

For the convenience in engineering applications the relationships among the drag coefficient, period parameter, and the Reynolds number are expressed in a mathematical form, based on the empirical data obtained from this study, as follows:

$$C_d = 15 P_e^{-0.5} \exp\left(\frac{1{\cdot}88}{R_e^{0.547}}\right), \tag{7}$$

where $P_e = U_m \tau / W$ denotes the period parameter and $R_e = U_m W \rho / \mu$ the Reynolds number. It must be noted that (7) is applicable for P_e ranging from 1·57 to 4·71 and R_e from 1·01 to 1057.

Figure 7 yields an expression of the relationship between the lift coefficient, C_m and the Reynolds number for a given period parameter. Due to the lack of sufficient analyzed data points available, the above expression is considered strictly qualitative.

REFERENCES

BATCHELOR, G. K. 1967 *An Introduction to Fluid Dynamics.* Cambridge University Press.

BRATER, E. F., MCNOWN, J. S. & STAIR, L. D. 1958 Waves forces on submerged structures. *J. Hyd. Div. ASCE* **1833**, 1–26.

BUCHANAN, H. J. 1968 Drag on flat plates oscillating in incompressible fluids at low Reynolds numbers. M.S. thesis, University of Alabama.

BUCHANAN, H. J. & BUGG, F. M. 1967 Orbital investigation of propellant dynamics in a large rocket booster. *NASA TN* D-3968. Washington: U.S. Govt. Printing Office.

COLE, H. A. & GAMBUCCI, B. J. 1961 Measured two-dimensional damping effectiveness of fuel sloshing baffles applied to ring baffles in cylindrical tanks. *NASA TN* D-694. Washington: U.S. Govt. Printing Office.

KEULEGAN, G. H. & CARPENTER, L. H. 1958 Forces on cylinders and plates in an oscillating fluid. *J. Res. Nat. Bur. Standards,* LX no. 5, 423–440.

LAMB, H. 1932 *Hydrodynamics.* New York: Dover.

MCNOWN, J. S. & KEULEGAN, G. H. 1959 Vortex formation and resistance in periodic motion. *J. Eng. Mech. Div. ASCE*, **1894**, 1–6.

MILES, J. W. 1958 Ring damping of free surface oscillations in a circular tank. *J. Appl. Mech. ASME*, **25**, 274–276.

MORRISON, J. R., O'BRIEN, M. P., JOHNSON, J. W. & SCHAFF, S. A. 1950 The force exerted by surface waves on piles. *J. Petroleum Tech.* **2**, 149–154.

SATTERLEE, H. M. & REYNOLDS, W. C. 1964 Dynamics of the free liquid surface in cylindrical containers under strong capillary and weak gravity conditions. *Stanford University Tech. Rep.* no. LG-2.

SCHWIND, R. G., SCOTTI, R. S. & SKOGH, J. 1964 Effect of baffles on tank sloshing. *Lockheed Missiles & Space Co.* LMSC-A64291.